Analysis and Evaluation of NASA's MK40B Six–Component Task Balance

N. Ulbrich†
Jacobs Technology Inc., Moffett Field, California 94035

The MK40B balance is NASA's newest balance of Task design. Its load range was optimized for use in the NASA Ames 11–ft Transonic Wind Tunnel. The balance was calibrated in 2019 in Calspan's Automatic Balance Calibration System. The data analysis was performed at the Ames Balance Calibration Laboratory. First, bi–directional characteristics of the six gage outputs of the balance were assessed by applying a semi–empirical test to the calibration data. These tests indicated that four of the six gages have bi–directional characteristics. Therefore, the use of absolute value terms in the regression models of the calibration data is justified. Then, the machine calibration data was analyzed using both the Non–Iterative and the Iterative Method. Analysis results for the two methods were compared using the percent contributions, the calibration load residuals, the primary sensitivities, and the principle linear terms. These results confirmed that the two methods describe bi–directional characteristics of the balance gages correctly. In addition, it was concluded that the load prediction accuracies of the two methods are the same for all practical purposes.

I. Nomenclature

$a_0, a_1, a_2, \ldots$	= coefficients of the regression model of a load component
AF	= axial force of a force balance
$b_0, b_1, b_2, \ldots$	= coefficients of the regression model of an output difference
D_i	= difference between the raw output and the natural zero of a balance gage
i	= balance gage index
$N1$	= forward normal force of a force balance
$N2$	= aft normal force of a force balance
rAF	= raw output of the axial force gage
$rAF_\circ$	= natural zero of the axial force gage
RM	= rolling moment of a force balance
$rN1$	= raw output of the forward normal force gage
$rN1_\circ$	= natural zero of the forward normal force gage
$rN2$	= raw output of the aft normal force gage
$rN2_\circ$	= natural zero of the aft normal force gage
rRM	= raw output of the rolling moment gage
$rRM_\circ$	= natural zero of the rolling moment gage
$rS1$	= raw output of the forward side force gage
$rS1_\circ$	= natural zero of the forward side force gage
$rS2$	= raw output of the aft side force gage
$rS2_\circ$	= natural zero of the aft side force gage
$S1$	= forward side force of a force balance
$S2$	= aft side force of a force balance
$\Delta S1$	= forward side force residual of a force balance
δD_3	= bi–directional part of the forward side force gage output difference

II. Introduction

Force balances of *Task* design have widely been used for load measurements on wind tunnel models for over 60 years. Data from a recent calibration of NASA's newest *Task* balance is used to discuss some

† Aerodynamicist, Jacobs Technology Inc.

of the pros and cons of its design. Two very positive traits of the *Task* design are its highly linear output and its relatively low gage interactions. On the other hand, *Task* balances have been known to develop hysteresis after its component parts become worn. In addition, some of the gages of a *Task* balance do exhibit *bi–directional* characteristics. These characteristics stem from design compromises that were made so that interactions could be kept at very low levels while still meeting expected load capacities for a given balance diameter. The term *bi–directional* describes the fact that the primary sensitivity of some of the gages of a *Task* balance depends on the sign of the related primary gage load. Consequently, the absolute value function must be used in the regression model of its calibration data so that *bi–directional* characteristics of the gage outputs are included in the load prediction equations. Despite all this, *Task* balances have proven themselves to be useful and accurate load measuring devices when properly maintained and calibrated.

It is helpful to review the use of the absolute value function during the analysis of *Task* balance data within the context of the two methods that are used in the aerospace testing community for the balance load prediction. First, the analysis of balance data using the *Iterative Method* is reviewed. This method fits the electrical outputs of the balance gages as a function of the balance loads. Afterwards, a load iteration equation is constructed from the coefficients of the fitted outputs so that loads can be predicted from outputs during a wind tunnel test. Four important ideas were originally suggested and/or developed by *Robin Galway* of *NRC Canada* that significantly improved description and analysis of balance calibration data whenever the *Iterative Method* is chosen for the definition of the load prediction equations:

• *Galway* suggested that the *natural zero* be used as the global datum for the electrical output of a balance gage (Ref. [1], p. 27; *Galway* uses the synonym *buoyant component offset* for the term *natural zero*).

• *Galway* suggested that the *absolute value of a load component* be included in the regression model of a gage output. Then, *bi–directional* characteristics of a gage output can be quantified (Ref. [1], pp. 21–23).

• *Galway* applied the *matrix solution*[†] of the least squares problem during the regression analysis of balance calibration data (Ref. [1], p. 13, Eq. (36)).

• *Galway* developed the *tare load iteration algorithm*. His algorithm was adopted by AIAA's *Internal Balance Technology Working Group* and first published in the open literature in 2003 (Ref. [4], 1st ed.).

In 2007, I observed that a direct connection between (i) the divergence of the load iterations and (ii) the presence of massive near–linear dependencies in the regression models of the gage outputs exists (see Ref. [5], p. 4 and Ref. [6], pp. 51–52). These unwanted dependencies result from the use of invalid terms that must be identified and removed before the final regression models of the gage outputs are generated. The *Variance Inflation Factor* may be used for this purpose (see Ref. [6], App. 18). The regression model of an output should only be used for the definition of the load iteration equation if the maximum of its *Variance Inflation Factor* set is below a recommended threshold. Suitable threshold values are given in the literature (see, e.g., Ref. [6], p. 369). The use of the *Variance Inflation Factor* for the detection of invalid terms has another advantage. The identification of invalid terms no longer depends on (i) an analyst's subject–matter knowledge or (ii) the observed convergence behavior of the load iterations (see related comments in Ref. [4], p. 16, 3rd para.). *Galway's* four ideas in combination with a systematic approach to identify invalid terms in the regression model of an output must be implemented in a balance data analysis tool if an analyst wants to reliably apply (i) global regression and (ii) the *Iterative Method* to *Task* balance data.

The *Non–Iterative Method* may also be used for the balance load prediction. This alternate approach directly fits a balance load as a function of the electrical outputs of the balance gages. Consequently, no iteration is needed to predict balance loads from electrical outputs during a wind tunnel test. I investigated the use of the *Non–Iterative Method* for the balance load prediction in great detail (see Ref. [6], App. 9, App. 12). Afterwards, I concluded that *Galway's* four ideas can also successfully be used with the *Non–Iterative Method* as long as two additional requirements are fulfilled:

• The electrical outputs of the balance gages are formatted as the difference between a raw output and the natural zero of a gage (see Ref. [6], App. 6, App. 9). Then, the *absolute value of an output difference* can be used to quantify *bi–directional* characteristics in the regression model of a load component.

• Invalid terms in the regression model of a load need to be identified and removed. Again, the *Variance Inflation Factor* may be used for this purpose (see Ref. [6], App. 18). A regression model of a load component

[†] The *matrix solution* was first proposed in 1956 by the British physicist *Roger Penrose* (see Refs. [2], [3]).

should only be used for data analysis and load prediction if the maximum of its *Variance Inflation Factor* set is below a literature recommended threshold (suitable threshold values are given in Ref. [6], p. 369).

Data from a machine calibration of NASA's MK40B balance is used in the next sections to illustrate characteristics of a *Task* balance. Afterwards, selected regression analysis results are examined and compared.

III. Balance Characteristics and Calibration

Machine calibration data of NASA's MK40B six–component force balance is used to illustrate the analysis of data from a *Task* balance with known *bi–directional* gage output characteristics. First, design features of the balance and the calibration load schedule are reviewed. Table 1 below summarizes important characteristics of the chosen balance and the given calibration data set of the MK40B balance.

Table 1: Overview of balance calibration data analysis example characteristics.

Balance Name (diameter)	Balance Design (load format)	Calibration Method	Comments
MK40B (2.50 inches)	force balance design $(N1, N2, S1, S2, AF, RM)$	machine calibration	normal & side force gage outputs are bi–directional

The MK40B balance belongs to a family of six–component balances of *Task* design that are manufactured by Aerophysics Research Instruments of Corona, California. Its load capacities are close to the expected load range of typical aircraft models that are tested in the NASA Ames 11–ft Transonic Wind Tunnel (TWT). Figure 1 below shows the overall layout of the MK40B balance. The MK40B balance is a

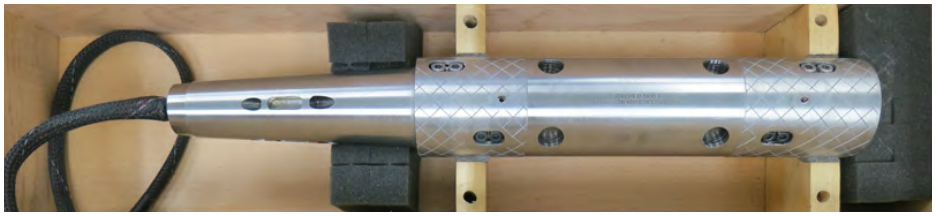

Fig. 1 Basic layout of NASA's 2.5 inch MK40B force balance.

multi–piece force balance. It measures five forces (forward & aft normal force, forward & aft side force, axial force) and one moment (rolling moment). These loads can easily be converted to direct–read format by applying load transformations that are listed in the literature (Ref. [6], App. 4). The balance has a cylindrical metric outer sleeve and a non–metric inner rod (diameter of the outer sleeve = 2.50 *in*; total length of the balance $\approx$ 11.0 *in*). Table 2 below lists capacities of the six load components of the balance

Table 2: Load capacities of the MK40B balance ($lbs \equiv$ pounds of force).

$N1$, lbs	$N2$, lbs	$S1$, lbs	$S2$, lbs	AF, lbs	RM, $in-lbs$
3500	3500	2500	2500	400	8000

in engineering units. The non–metric part of the balance is typically mounted on a sting that is attached to the rear model support strut of the Ames 11–ft TWT.

The calibration of the balance was performed in Calspan's Automatic Balance Calibration System (ABCS). The chosen calibration load schedule consisted of 1646 data points that were distributed across 17 load series. Up to three load components were simultaneously applied during the machine calibration.

The natural zeros of the balance gages are the electrical outputs that the balance would have in a weightless condition. Their determination is briefly discussed in the next section. Then, *bi–directional* characteristics of the balance gage are assessed. Finally, selected analysis results are presented that were obtained after the application of the *Non–Iterative* and the *Iterative Method* to the calibration data.

IV. Natural Zero Determination

The natural zeros are important physical constants of a strain–gage balance. They are the raw electrical outputs that the balance gages have when the balance is in a weightless condition. The natural zeros are

often used as a global output datum so that all outputs can be described as output differences relative to a fixed reference. Then, small instrumentation dependent bias errors can be removed from the outputs as long as the raw outputs and the natural zeros are measured using the same instrumentation setup.

Different techniques may be used to determine the natural zeros of a balance (see Ref. [6], App. 8). In this instance, the balance was placed on a leveling table using V–blocks and oriented such that the negative normal force was pointing in the direction of the gravitational acceleration. Then, raw outputs were recorded. Afterwards, the balance was rotated by 90 deg, 180 deg, and 270 deg. All these orientations resulted in four independent sets of raw output readings. The numerical process of averaging cancels the influence of any gravity load on the gage outputs as, by design, the average of the loads of all four orientations is zero. The natural zeros of the six gages are simply the averages of the outputs of the four balance orientations. Table 3 below shows the measured raw outputs and the final natural zeros of the balance.

Table 3: Calculation of the natural zeros of the MK40B balance.

Orientation (roll angle)	$rN1_\circ$ microV/V	$rN2_\circ$ microV/V	$rS1_\circ$ microV/V	$rS2_\circ$ microV/V	$rAF_\circ$ microV/V	$rRM_\circ$ microV/V	Applied Loads $U, V, W, X = forces$
0°	−21.54	−6.08	+8.31	−9.68	−145.41	−8.05	$N1 = -U\ ;\ N2 = -V$
90°	−15.76	−1.18	+0.13	−16.08	−145.20	−8.41	$S1 = -W\ ;\ S2 = -X$
180°	−9.81	+3.82	+8.59	−9.22	−145.17	−9.09	$N1 = +U\ ;\ N2 = +V$
270°	−15.66	−1.14	+16.73	−2.65	−145.13	−8.69	$S1 = +W\ ;\ S2 = +X$
Natural Zero†	−15.69	−1.15	+8.44	−9.41	−145.23	−8.56	*Load Average*‡ = 0

†Natural zero = arithmetic mean of the column values. ‡By design, AF and RM are zero for all orientations.

In theory, the natural zeros are repeatable physical constants as long as (i) no changes to both wiring and gaging of the balance are made, (ii) the balance does not experience plastic deformation during use, and (iii) the same hardware setup is used for the measurement of the electrical outputs. – The *bi–directional* characteristics of the gage outputs of the balance are investigated in detail in the next section.

V. Bi–directional Output Characteristics

A semi–empirical test for the evaluation of the *bi–directional* output characteristics of a gage was developed at the Ames Balance Calibration Laboratory (Ref. [6], App. 7). The test makes it possible to quantify *bi–directional* characteristics. It works with both the *Non–Iterative* and the *Iterative Method*. The test was developed because it is difficult to assess *bi–directional* output characteristics simply by plotting the measured outputs versus the related primary load component. The change in slope from positive to negative loading at this scale is, for all practical purposes, invisible. Two conditions need to be met for a gage to be *bi–directional*: (i) the absolute value of the *bi–directional* part of the output at capacity must exceed the output threshold of the gage and (ii) the p–value of the absolute value term must be less than 0.001.

Table 4 below shows test results for each gage output of the MK40B balance that were obtained after the application of the *Non–Iterative Method* to the given machine calibration data. Absolute value terms of the output differences relative to the natural zeros were temporarily included in the regression models of the balance loads so that the test could be performed. The first row lists the empirical output threshold for each gage output. It equals 0.5 % of the maximum output at load capacity of the gage. The second row has

Table 4: *Non–Iterative Method* $\Longrightarrow$ Test results for the MK40B balance.

	$rN1$	$rN2$	$rS1$	$rS2$	rAF	rRM
output threshold, microV/V	$T = 6.89$	$T = 8.35$	$T = 7.00$	$T = 7.46$	$T = 8.46$	$T = 7.29$
|bi–directional part|, microV/V	$4.75 < T$	$13.21 > T$	$16.89 > T$	$13.88 > T$	$5.21 < T$	$1.68 < T$
p–value of absolute value term	< 0.001	< 0.001	< 0.001	< 0.001	< 0.001	< 0.001
Is output bi–directional ?	NO	**YES**	**YES**	**YES**	NO	NO

the absolute value of the computed *bi–directional* part of the output at capacity (Ref. [6], App. 7, Eq. (7.4a)). The third row has the p–values of the principle absolute value terms of the regression models of the loads.

It is observed that three of the six outputs fulfill both conditions that are needed for an output to be *bi–directional*. Therefore, the use of absolute value terms of the related three gage output differences in the final regression models of the loads can be justified if the *Non–Iterative Method* is applied.

It is interesting to compare the predicted *bi–directional* parts at load capacity that are computed using the regression models of the loads (Ref. [6], App. 7, Eq. (7.4a)) with values that are obtained using the regression models of the output differences (Ref. [6], App. 7, Eq. (7.7a)). Table 5 below lists corresponding values for the MK40B balance. The agreement between the predicted values is excellent. This result is no

Table 5: Comparison of bi–directional parts at capacity for the MK40B balance.

	$rN1$ microV/V	$rN2$ microV/V	$rS1$ microV/V	$rS2$ microV/V	rAF microV/V	rRM microV/V
Non–Iterative Method	+4.75	+13.21	+16.89	+13.88	+5.21	−1.68
Iterative Method	+5.12	+11.38	+16.49	+13.38	+5.22	−1.70

surprise because the *bi–directional* part of the output at capacity is a true physical property. Therefore, it must be independent of the method that is used for the analysis of the calibration data.

Figure 2 below shows the forward side force gage output difference (D_3) plotted versus the tare corrected forward side force ($S1$) of the MK40B balance. The plot was obtained during the regression analysis of the calibration data with the *Non–Iterative Method*. The outputs range from approximately

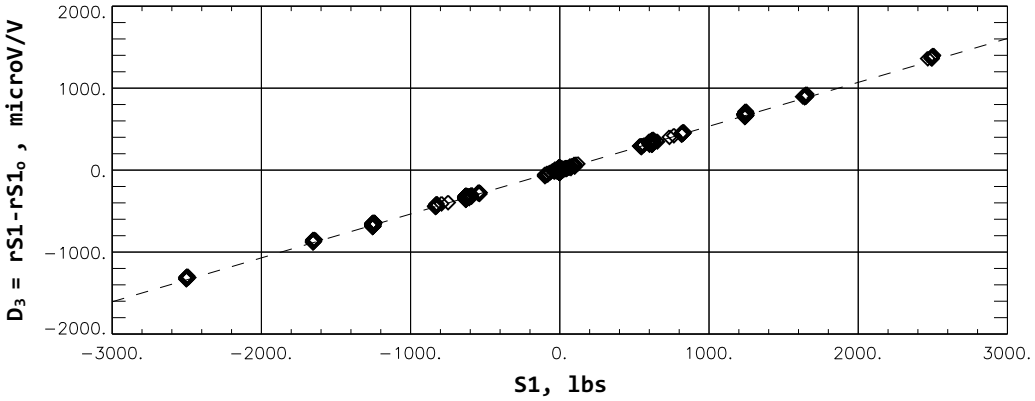

Fig. 2 Forward side force gage output difference plotted versus the forward side force.

−1400 to +1400 $microV/V$ if the negative and positive values of the forward side force capacity are used as boundaries. Figure 3 shows the *bi–directional* part of the forward side force gage output difference plotted

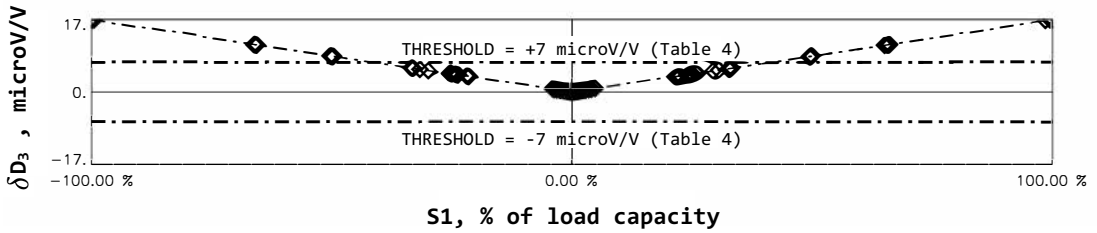

Fig. 3 The bi–directional part of the forward side force gage output difference plotted versus the forward side force that is expressed as a percentage of capacity.

versus the forward side force. The absolute value of the *bi–directional* part at capacity was estimated to be 16.89 $microV/V$ (see Table 5 above). It is about 1.2 % of the output at load capacity. Consequently,

bi–directional properties of the forward side force gage output are significant. This conclusion is based upon experience gained after the analysis of data from a large number of Task balances. The *bi–directional* behavior is significant but still very small when compared with the overall range of the forward side force gage output difference. Consequently, it cannot be detected by visual examination if an analyst simply plots the forward side force gage output difference versus the forward side force (compare Fig. 2 with Fig. 3).

It is helpful to identify the most likely root cause of the *bi–directional* characteristic of a balance gage in order to gain confidence in the chosen regression model's ability to describe the physical behavior of the balance. The *bi–directional* characteristic can be interpreted as an asymmetry in the gage sensitivity if a gage output is plotted versus the related load component. This asymmetry may be associated with a geometric asymmetry that is hidden in design features of the balance. Figure 4 below shows, for example, parts of a typical *Task* balance. The balance has a metric outer sleeve. It is the physical interface to the wind tunnel model. The balance also has a non–metric inner rod. It is the interface to the balance support system. Circumferential wall thickness variations of both the outer sleeve and inner rod can clearly be seen. They

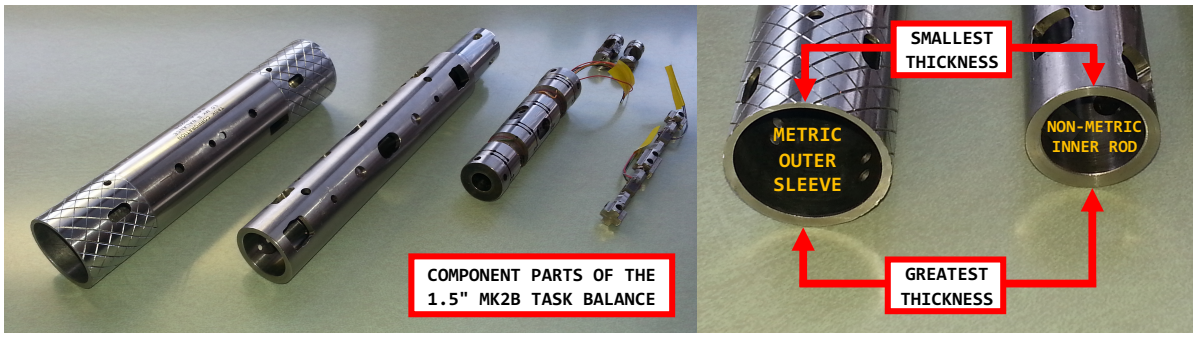

Fig. 4 Wall thickness variations of the metric and non–metric parts of a *Task* balance.

are a known design feature of *Task* balances. The wall thickness variations may be responsible for a change of the elastic behavior of the balance. In that context, *Hufnagel* makes the following comments (taken from Ref. [7], pp. 236–237; *Able type balances* ≡ *Task type balances*):

. . . Asymmetric sensitivity is a special problem of the Able type balances (p. 236) . . . The main reason for the asymmetric sensitivity behavior is found in the asymmetric wall thickness distribution of the inner and outer tubes. This asymmetry results in a difference in the deformation of tubes for positive and negative loading. The effect was detected by comparison of a balance with central and eccentric wall distributions. (p. 237) . . .

The change of the elastic behavior is detected whenever (i) a force is applied perpendicular to the roll axis and (ii) the force changes sign. These forces are the forward & aft normal forces and the forward & aft side forces. The change of the elastic behavior is observed as a slope change when an output is plotted versus the related primary load component. The change is modeled during the analysis of balance calibration data by superimposing the effects of linear and absolute value terms in the chosen regression models.

Magnitudes of the circumferential wall thickness variations of a *Task* balance are highly dependent on the load capacities of the balance. It was observed over the years that the magnitudes of the *bi–directional* characteristic of the two normal force gages and the two side force gages are often very close in magnitude. However, magnitudes of the *bi–directional* output at capacity of the side force gage pair are often higher than corresponding values for the normal force gage pair. These observations clearly point towards a direct connection between the *bi–directional* characteristics of the normal and side force gages and the circumferential wall thickness variations of the metric and non–metric component parts of a *Task* balance.

It is useful to compare the magnitude of the *bi–directional* part at load capacity for a family of *Task* balances in order to better support these conclusions. Therefore, both the *Non–Iterative Method* and the *Iterative Method* were applied to calibration data of NASA's MK29B, MK40A, and MK4A balances so that an estimate of the *bi–directional* part at load capacity could be computed by using both Eq. (7.4*a*) and Eq. (7.7*a*) that are given in Ref. [6]. Table 6 below lists results for the three balances. The first value in

Table 6: Bi–directional parts at load capacity for a family of *Task* balances.

Balance (diameter)	Analysis Method	$rN1$ microV/V	$rN2$ microV/V	$rS1$ microV/V	$rS2$ microV/V	rAF microV/V	rRM microV/V
MK29B (2.0 in)	Non–Iterative Method	+7.65	+10.68	+12.45	+18.52	+0.14	–1.41
	Iterative Method	+7.30	+9.81	+10.89	+18.46	+0.17	+1.63
MK40A (2.5 in)	Non–Iterative Method	+10.07	+13.49	+23.12	+24.70	+0.33	–1.33
	Iterative Method	+10.63	+12.71	+22.53	+23.76	+0.32	–1.26
MK4A (4.0 in)	Non–Iterative Method	+4.78	+7.75	+7.53	+4.58	+0.02	–0.27
	Iterative Method	+4.82	+7.58	+7.38	+4.80	+0.00	–0.35

each box was obtained after applying Eq. (7.4*a*) of Ref. [6]. This equation uses coefficients of the regression models of the tare corrected balance loads as input. The second value in each box was obtained after applying Eq. (7.7*a*) of Ref. [6]. This alternate equation uses coefficients of the regression models of the gage output differences as input. Several observations can be made after examining Table 6 in more detail. First, values for Eq. (7.4*a*) and Eq. (7.7*a*) show excellent agreement even though they were obtained by using coefficients of fundamentally different regression models as input. In most cases, the agreement between the values is on the order of 1.0 *microV/V* or better. It can also be seen that the magnitude of the values for the normal and side force gages are significantly larger than the magnitude of the values for the rolling moment and axial force gages. This result confirms that *bi–directional* characteristics of the normal and side force gages of a *Task* balance are most likely caused by circumferential wall thickness variations.

VI. Analysis Results for the Non–Iterative Method

The *Non–Iterative Method* is used in this section for the development of the load prediction equations of the MK40B balance. This approach directly fits the six balance load components, i.e., $N1$, $N2$, $S1$, $S2$, AF, and RM as a function of the gage output differences D_1, D_2, ..., D_6 assuming that all balance loads are described relative to the absolute load datum of zero load (for more detail see Ref. [6], App. 9). Table 7 below shows the upper bound of all 85 terms that were considered for the regression models. It was decided

Table 7: Upper bound of the regression model terms of a *load component* of the MK40B balance.

Intercept Term (1 possible term)
Linear Terms (6 possible terms)[†] $D_1,\ D_2,\ D_3,\ D_4,\ D_5,\ D_6$
Absolute Value Terms (6 possible terms) $\lvert D_1\rvert,\ \lvert D_2\rvert,\ \lvert D_3\rvert,\ \lvert D_4\rvert,\ \lvert D_5\rvert,\ \lvert D_6\rvert$
Quadratic Terms (6 possible terms) $D_1^2,\ D_2^2,\ D_3^2,\ D_4^2,\ D_5^2,\ D_6^2$
Linear $\times$ Absolute Value Terms (6 possible terms) $D_1 \cdot \lvert D_1\rvert,\ D_2 \cdot \lvert D_2\rvert,\ D_3 \cdot \lvert D_3\rvert,\ D_4 \cdot \lvert D_4\rvert,\ D_5 \cdot \lvert D_5\rvert,\ D_6 \cdot \lvert D_6\rvert$
Cross–product Terms (60 possible terms) $(D_1 \cdot D_2)\ ,\ (D_1 \cdot D_3)\ ,\ (D_1 \cdot D_4)\ ,\ \ldots\ ,\ \lvert D_5 \cdot D_6\rvert$

[†] $D_1 = rN1 - rN1_\circ$, $D_2 = rN2 - rN2_\circ$, $D_3 = rS1 - rS1_\circ$, $D_4 = rS2 - rS2_\circ$, $D_5 = rAF - rAF_\circ$, $D_6 = rRM - rRM_\circ$

to include absolute value terms of all gages in the list of possible terms even though the outputs of the forward normal force, axial force, and rolling moment gage did not show *bi–directional* characteristics (see Table 5). This choice was made because the semi–empirical test cannot capture more complex *bi–directional* characteristics (see related comments in Ref. [6], App. 7, section 7.5). A simplified regression model search algorithm was used for the selection of the terms of each load component (the search algorithm is described in Ref. [6], App. 19). The search was successfully completed for all six load components. Afterwards, global regression was applied so that the coefficients of the chosen terms could be determined.

Figure 5 below shows percent contributions of the thirty–six principle linear terms and the thirty–six principle absolute value terms of the regression models of the six load components (for simplicity, percent

	N1	N2	S1	S2	AF	RM
D1	[100.00 %]	+10.72 %	−2.67 %	−0.50 %	+0.45 %	+0.17 %
D2	+2.70 %	[100.00 %]	−0.18 %	−3.10 %	−0.56 %	−0.14 %
D3	−0.11 %	−0.69 %	[100.00 %]	+4.34 %	+0.54 %	+0.03 %
D4	−0.13 %	+0.29 %	+1.37 %	[100.00 %]	−0.61 %	+0.06 %
D5	0	0	0	0	[100.00 %]	+0.08 %
D6	+0.14 %	+0.33 %	−2.47 %	−2.03 %	+3.54 %	[100.00 %]
ID1I	−0.42 %	−0.43 %	+0.99 %	+0.12 %	−0.15 %	−0.01 %
ID2I	−0.65 %	−0.87 %	+0.04 %	+1.17 %	−0.26 %	−0.20 %
ID3I	+0.23 %	+0.17 %	−1.66 %	−0.30 %	+0.03 %	−0.02 %
ID4I	+0.12 %	+0.25 %	−0.27 %	−1.21 %	−0.06 %	+0.01 %
ID5I	0	0	−0.01 %	0	−0.11 %	0
ID6I	+0.33 %	+0.28 %	−1.43 %	−0.31 %	−1.33 %	+0.12 %

Interpretation of the Percent Contribution (taken from Ref. [5], App. 16)

Percent_Contribution = 100 % ..... primary/reference term (red)
ABS(Percent_Contribution) > 0.5 % ..... very important term (red)
0.1 % < ABS(Percent_Contribution) < 0.5 % ... term of minor importance (blue)
ABS(Percent_Contribution) < 0.1 % ..... term of no importance (black)

Fig. 5 Percent contributions of the principle linear and absolute value terms of the fitted *balance load components*.

contributions of higher order terms are not discussed). Red color marks percent contributions of very important terms. Blue color is used to identify terms that are of minor importance. Finally, black color is used to mark terms of no importance. In general, it can be seen that interactions and *bi–directional* characteristics of the gages cannot be neglected. A total of 21 of the 72 terms are highlighted in red color (not counting the percent contribution of 100 %). These 21 terms are very important terms as the magnitude of their percent contributions exceeds the empirical threshold of 0.5 %.

It is also interesting to examine the relationship between the forward side force ($S1$) and the rolling moment gage output difference (D_6). The rolling moment gage output difference (D_6) is needed in the regression model of the forward side force ($S1$) as a connection between the rolling moment gage output (D_6) and the forward side force ($S1$) exists. The percent contribution of the term D_6 of the regression model of $S1$ has the relatively large value of $-2.47\,\%$. In addition, it is known that the connection between the rolling moment gage output (D_6) and the forward side force ($S1$) is *bi–directional*. This relationship is reflected in Fig. 5 above by the fact that the percent contribution of the term $|D_6|$ also has the relatively large value of $-1.43\,\%$.

A tare load iteration was performed during the calibration data analysis so that balance loads resulting from the combined weight of the load adapter of the calibration machine and the metric part of the balance would be included in the load set that was ultimately used as input for the regression analysis (Ref. [6], App. 12 describes the tare load iteration algorithm that the *Non–Iterative Method* uses).

The regression analysis of the data was successfully completed using (i) tare corrected loads and (ii) output differences relative to the natural zeros of the balance gages as input. Table 8 below lists the standard deviation of the load residuals, i.e., of the difference between measured and fitted load, for each load component of the MK40B balance. The standard deviations of all load components are near or below the threshold of 0.1 % of load capacity that is used in the aerospace testing community for the assessment of the standard deviation of balance load residuals.

Table 8: *Non–Iterative Method* $\Longrightarrow$ Standard deviation of the load residuals.[†]

$N1$ *lbs*	$N2$ *lbs*	$S1$ *lbs*	$S2$ *lbs*	AF *lbs*	RM *in−lbs*
2.16 (0.062 %)	2.32 (0.066 %)	2.70 (0.108 %)	2.93 (0.117 %)	0.45 (0.112 %)	2.87 (0.036 %)

[†]Standard deviations expressed as a percentage of the load capacity are listed in brackets.

As an example, forward side force residuals of the MK40B balance are plotted versus the tare corrected forward side force in Fig. 6 below. Most residuals are well within the threshold of $\pm 0.25\,\%$ of load capacity

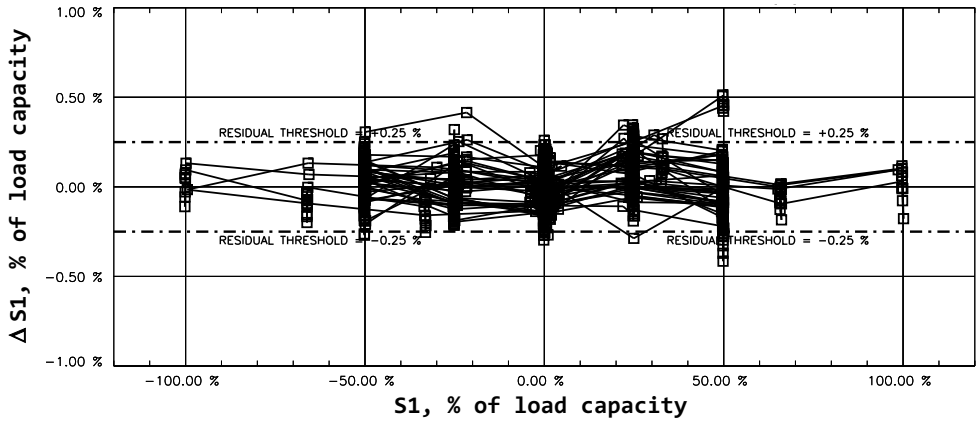

Fig. 6 *Non–Iterative Method* $\Longrightarrow$ Forward side force residuals ($\Delta S1$) of the MK40B balance plotted versus the tare corrected forward side force ($S1$).

that is often used for the assessment of individual load residuals. A few outliers are detected that exceed the threshold of ± 0.25 %. The primary sensitivities of the balance gages were also computed during the regression analysis of the calibration data. The primary sensitivity of a balance gage equals the first derivative of a gage output with respect to the corresponding primary gage load. Therefore, it can be approximated by the inverse of the coefficient of the primary output difference that is used in the regression model of a load if the *Non–Iterative Method* is used for the balance load prediction. This statement can be illustrated by using the regression model of the forward normal force as an example. It is defined as follows:

$$N1 \;=\; a_\circ \;+\; a_1 \cdot \overbrace{(rN1 - rN1_\circ)}^{D_1} \;+\; a_2 \cdot \overbrace{(rN2 - rN2_\circ)}^{D_2} \;+\; a_3 \cdot \overbrace{(rS1 - rS1_\circ)}^{D_3} \;+\; \ldots \qquad (1)$$

Then, the inverse of the primary sensitivity of the forward normal force gage output is obtained:

$$a_1 \;=\; \frac{\partial\, N1}{\partial\, D_1} \;\approx\; \left\{ \frac{\partial\, D_1}{\partial\, N1} \right\}^{-1} = \left\{ \frac{\partial\, [\, rN1 - \overbrace{rN1_\circ}^{const.}\,]}{\partial\, N1} \right\}^{-1} = \left\{ \frac{\partial\, rN1}{\partial\, N1} \right\}^{-1} \qquad (2)$$

Consequently, the primary sensitivity of the forward normal force gage output becomes:

$$\begin{array}{c} Primary\ Sensitivity \\ (forward\ normal\ force\ gage) \end{array} \quad \Longrightarrow \quad \frac{\partial\, rN1}{\partial\, N1} \;\approx\; \frac{1}{a_1} \qquad (3)$$

Table 9 below lists the primary sensitivities of the MK40B balance. As expected, the axial force gage has the highest sensitivity of all balance gages because the axial force capacity is about one order of magnitude below the normal and side force capacities.

Table 9: *Non–Iterative Method* $\Longrightarrow$ Primary sensitivities of the MK40B balance.

$\frac{\partial\, rN1}{\partial\, N1}$	$\frac{\partial\, rN2}{\partial\, N2}$	$\frac{\partial\, rS1}{\partial\, S1}$	$\frac{\partial\, rS2}{\partial\, S2}$	$\frac{\partial\, rAF}{\partial\, AF}$	$\frac{\partial\, rRM}{\partial\, RM}$
$0.3944^\dagger$	$0.4406^\dagger$	$0.5355^\dagger$	$0.5560^\dagger$	$4.2340^\dagger$	$0.1823^\ddagger$

$^\dagger [microV/V]\,/\,[lbs]$; $^\ddagger [microV/V]\,/\,[in\text{–}lbs]$.

Table 10 below lists the subset of the thirty–six principle linear coefficients of the regression models of the six load components of the MK40B balance. These coefficient values will be compared at the end of the

Table 10: *Non–Iterative Method* $\Longrightarrow$ Principle linear coefficients of the fitted regression model of each balance load component.

	N1	N2	S1	S2	AF	RM
D1	2.535300e+00	2.780104e-01	-4.980264e-02	-8.989443e-03	1.303604e-03	9.887143e-03
D2	5.986084e-02	2.269841e+00	-2.986586e-03	-4.878903e-02	-1.408642e-03	-7.171038e-03
D3	-2.786888e-03	-1.781739e-02	1.867544e+00	7.807798e-02	1.548382e-03	1.901659e-03
D4	-3.279444e-03	7.642063e-03	2.553950e-02	1.798494e+00	-1.758750e-03	3.441410e-03
D5	0.000000e+00	0.000000e+00	0.000000e+00	0.000000e+00	2.361830e-01	3.777998e-03
D6	3.338612e-03	8.013759e-03	-4.305346e-02	-3.405238e-02	9.465577e-03	5.484038e+00

next section with corresponding values that were obtained after the application of the *Iterative Method*.

VII. Analysis Results for the Iterative Method

The *Iterative Method* is used in this section for calibration data analysis and the load prediction of the MK40B balance (see Ref. [4] or Ref. [6], App. 10 for a detailed description of the method). This alternate approach first fits the electrical outputs of the balance gages as a function of the balance loads. Afterwards, a load iteration equation is constructed from the regression coefficients of the fitted outputs so that loads can be predicted from measured outputs during a wind tunnel test. Finally, iteration equation coefficients are stored in a standardized data reduction matrix so that the iteration equation can easily be shared and/or implemented in the data system of a wind tunnel.

Table 11 below shows the upper bound of all 85 terms that were considered for the regression models of the six gage output differences D_1, D_2, ..., D_6. It is assumed that all balance loads are described relative to the absolute load datum of zero load. Again, it was decided to include all possible absolute value terms in the upper bound so that more complex *bi–directional* characteristics can be modeled. Then, a simplified regression model search algorithm was applied to the given calibration data (the algorithm was also used during the application of the *Non–Iterative Method* ; it is described in Ref. [6], App. 19). The search was

Table 11: Upper bound of the regression model terms of an *output difference*† of the MK40B balance.

Intercept Term (1 possible term)
Linear Terms (6 possible terms)† $N1,\ N2,\ S1,\ S2,\ AF,\ RM$
Absolute Value Terms (6 possible terms) $\lvert N1\rvert,\ \lvert N2\rvert,\ \lvert S1\rvert,\ \lvert S2\rvert,\ \lvert AF\rvert,\ \lvert RM\rvert$
Quadratic Terms (6 possible terms) $N1^2,\ N2^2,\ S1^2,\ S2^2,\ AF^2,\ RM^2$
Linear $\times$ Absolute Value Terms (6 possible terms) $N1\cdot\lvert N1\rvert,\ N2\cdot\lvert N2\rvert,\ S1\cdot\lvert S1\rvert,\ S2\cdot\lvert S2\rvert,\ AF\cdot\lvert AF\rvert,\ RM\cdot\lvert RM\rvert$
Cross–product Terms (60 possible terms) $(N1\cdot N2)\ ,\ (N1\cdot S1)\ ,\ (N1\cdot S2)\ ,\ \ldots\ ,\ \lvert AF\cdot RM\rvert$

$^{\dagger}D_1{=}rN1{-}rN1_{\circ}\ ,\ D_2{=}rN2{-}rN2_{\circ}\ ,\ D_3{=}rS1{-}rS1_{\circ}\ ,\ D_4{=}rS2{-}rS2_{\circ}\ ,\ D_5{=}rAF{-}rAF_{\circ}\ ,\ D_6{=}rRM{-}rRM_{\circ}$

successfully completed for all six output differences. Afterwards, global regression was applied so that the coefficients of the chosen terms could be determined and the load iteration equation could be derived.

Percent contributions of the regression model terms were determined after completion of the regression analysis of the calibration data. Figure 7 below shows the percent contributions of the thirty–six principle linear terms and the thirty–six principle absolute value terms of the regression models of the six gage output differences (for simplicity, percent contributions of higher order terms are not discussed). Red color marks percent contributions of very important terms. Blue color is used to identify terms that are of minor importance. Finally, black color is used to mark terms of no importance. In general, it can be seen that the interactions between the gages cannot be neglected. A total of 22 of the 72 terms are highlighted in red color (not counting the percent contribution of 100 %). These 22 terms are considered to be very important

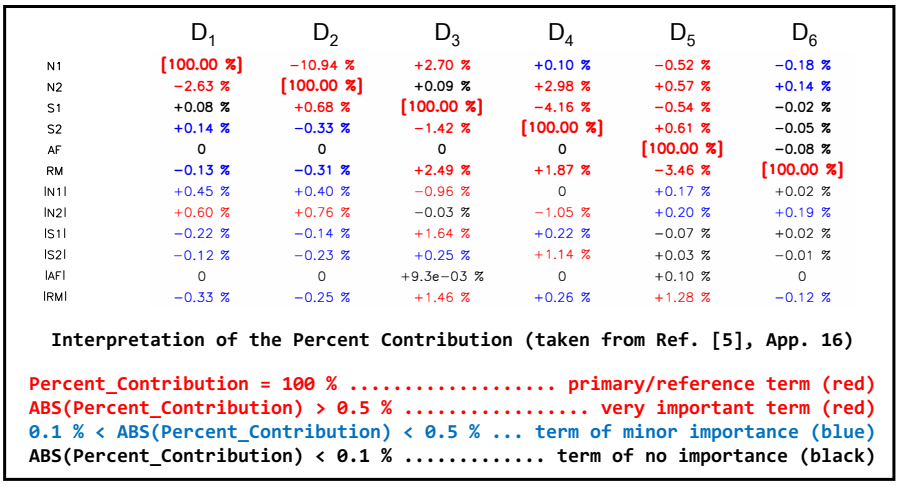

	D_1	D_2	D_3	D_4	D_5	D_6
N1	[100.00 %]	−10.94 %	+2.70 %	+0.10 %	−0.52 %	−0.18 %
N2	−2.63 %	[100.00 %]	+0.09 %	+2.98 %	+0.57 %	+0.14 %
S1	+0.08 %	+0.68 %	[100.00 %]	−4.16 %	−0.54 %	−0.02 %
S2	+0.14 %	−0.33 %	−1.42 %	[100.00 %]	+0.61 %	−0.05 %
AF	0	0	0	0	[100.00 %]	−0.08 %
RM	−0.13 %	−0.31 %	+2.49 %	+1.87 %	−3.46 %	[100.00 %]
|N1|	+0.45 %	+0.40 %	−0.96 %	0	+0.17 %	+0.02 %
|N2|	+0.60 %	+0.76 %	−0.03 %	−1.05 %	+0.20 %	+0.19 %
|S1|	−0.22 %	−0.14 %	+1.64 %	+0.22 %	−0.07 %	+0.02 %
|S2|	−0.12 %	−0.23 %	+0.25 %	+1.14 %	+0.03 %	−0.01 %
|AF|	0	0	+9.3e−03 %	0	+0.10 %	0
|RM|	−0.33 %	−0.25 %	+1.46 %	+0.26 %	+1.28 %	−0.12 %

Interpretation of the Percent Contribution (taken from Ref. [5], App. 16)

Percent_Contribution = 100 % ..... primary/reference term (red)
ABS(Percent_Contribution) > 0.5 % ..... very important term (red)
0.1 % < ABS(Percent_Contribution) < 0.5 % ... term of minor importance (blue)
ABS(Percent_Contribution) < 0.1 % ..... term of no importance (black)

Fig. 7 Percent contributions of the principle linear and absolute value terms of the six fitted *output differences*.

terms as the magnitude of their percent contributions exceeds the threshold of 0.5 %. More complex *bi–directional* connections between load components and output differences were detected. It is interesting to examine the relationship between the forward side force gage output difference (D_3) and the rolling moment (RM). The rolling moment (RM) is needed in the regression model of the forward side force gage output difference (D_3) as a connection between the rolling moment and the forward side force gage output difference exists. Therefore, the percent contribution of the rolling moment (RM) of the regression model of the forward side force gage output difference (D_3) has the relatively large value of +2.49 %. In addition, it is known that the connection between the rolling moment (RM) and the forward side force gage output difference (D_3) is *bi–directional*. This relationship is reflected in Fig. 7 above by the fact that the percent contribution of the absolute value of the rolling moment ($|RM|$) has the relatively large value of +1.46 %.

It is proven in the literature that the following connection between the percent contributions of the regression models of the loads and output differences exists (see Ref. [6], pp. 353–355): → *Percent contributions of pairs of related terms are similar in magnitude but opposite in sign.* This connection can be illustrated by using percent contributions as an example that were discussed in the previous paragraph. First, it is known from the regression model of the forward side force gage output difference (D_3) that (i) the percent contribution of the rolling moment (RM) equals +2.49 % and (ii) the percent contribution of the absolute value of the rolling moment ($|RM|$) equals +1.46 % (taken from Fig. 7). Now, the *Non–Iterative Method* is used instead of the *Iterative Method* for the calibration data analysis. Consequently, the forward side force ($S1$) is the term that is related to the forward side force gage output difference (D_3). Similarly, the rolling moment gage output difference (D_6) is the term that is related to the rolling moment (RM). Then, it known from the regression model of the forward side force (S_1) that (i) the percent contribution of the rolling moment gage output difference (D_6) equals −2.47 % and (ii) the percent contribution of the absolute value of the rolling moment gage output difference ($|D_6|$) equals −1.43 % (values were copied from Fig. 5). As expected, the percent contribution of D_6 is similar in magnitude but opposite in sign to the percent contribution of RM (−2.47 % versus +2.49 %). Likewise, the percent contribution of $|D_6|$ is similar in magnitude but opposite in sign to the percent contribution of $|RM|$ (−1.43 % versus +1.46 %).

A tare load iteration was performed during the calibration data analysis so that balance loads resulting from the combined weight of the load adapter of the calibration machine and the metric part of the balance would be included in the load set that was ultimately used for the regression analysis (Ref. [6], App. 13 describes the tare load iteration algorithm that the *Iterative Method* uses).

The regression analysis of the data was successfully completed using (i) the tare corrected loads and (ii) output differences relative to the natural zeros of the balance as input. Afterwards, a data reduction matrix for the load prediction was generated that has the coefficients of the load iteration equation. Table 12 below lists the standard deviation of the load residuals of the calibration data, i.e., of the difference between measured and predicted load, for each load component of the MK40B balance in engineering units (correspond-

ing values expressed as a percentage of the capacity are listed in brackets). The standard deviations of the predicted loads are near or below the threshold of 0.1 % that is used in the aerospace testing community

Table 12: *Iterative Method* $\Longrightarrow$ Standard deviation of the load residuals.[†]

$N1$ lbs	$N2$ lbs	$S1$ lbs	$S2$ lbs	AF lbs	RM $in-lbs$
2.13 (0.061 %)	2.37 (0.068 %)	2.70 (0.108 %)	2.97 (0.119 %)	0.46 (0.115 %)	2.95 (0.037 %)

[†]Standard deviations expressed as a percentage of the load capacity are listed in brackets.

for the assessment of the standard deviation of balance load residuals. The standard deviations shown in Table 12 can be compared with corresponding values that are listed in Table 8 for the *Non–Iterative Method*. The maximum difference between the standard deviations is very small (≈ 0.003 %). Therefore, it is concluded that the standard deviation of the load residuals show excellent agreement with corresponding values that were obtained after the application of the *Non–Iterative Method*.

As an example, forward side force residuals of the MK40B balance are plotted versus the tare corrected forward side force in Fig. 8 below. Most load residuals are well within the threshold of ± 0.25 % of the load

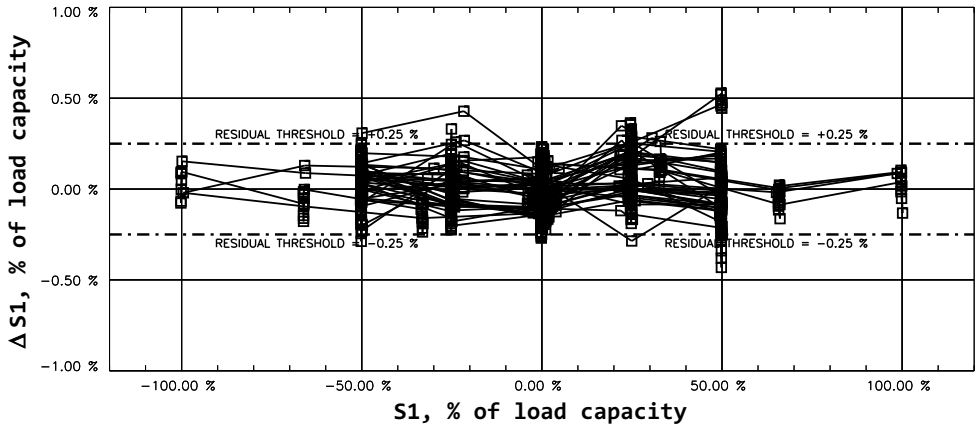

Fig. 8 *Iterative Method* $\Longrightarrow$ Forward side force residuals ($\Delta S1$) of the MK40B balance plotted versus the tare corrected forward side force ($S1$).

capacity. Again, plotted load residuals show excellent qualitative and quantitative agreement with corresponding values that are shown in Fig. 6 for the *Non–Iterative Method*.

The primary sensitivities of the balance gages were also computed during the regression analysis of the calibration data. In this context, the primary sensitivity of a gage is defined as the coefficient of the primary load component that is used in the regression model of a gage output difference. This general statement can be illustrated by using the regression model of the gage output difference D_1 of the forward normal force gage as an example. This regression model is defined in Eq. (4) below. The primary sensitivity of output

$$D_1 \;=\; rN1 \;-\; rN1_\circ \;=\; b_\circ \;+\; b_1 \cdot N1 \;+\; b_2 \cdot N2 \;+\; b_3 \cdot S1 \;+\; b_4 \cdot S2 \;+\; \ldots \tag{4}$$

difference D_1 equals the coefficient of the forward normal force. Then, we get:

$$\begin{array}{c} \textit{Primary Sensitivity} \\ (\textit{forward normal force gage}) \end{array} \quad \Longrightarrow \quad b_1 \;=\; \frac{\partial\, D_1}{\partial\, N1} \;=\; \frac{\partial\, [\, rN1 - \overbrace{rN1_\circ}^{const.}\,]}{\partial\, N1} \;=\; \frac{\partial\, rN1}{\partial\, N1} \tag{5}$$

Table 13 below lists the primary sensitivities for the MK40B balance. Again, the axial force gage has the highest sensitivity of all balance gages because the axial force capacity is about one order of magnitude

below the capacities of the normal and side forces.

Table 13: *Iterative Method* $\Longrightarrow$ Primary sensitivities of the MK40B balance.

$\frac{\partial\, rN1}{\partial\, N1}$	$\frac{\partial\, rN2}{\partial\, N2}$	$\frac{\partial\, rS1}{\partial\, S1}$	$\frac{\partial\, rS2}{\partial\, S2}$	$\frac{\partial\, rAF}{\partial\, AF}$	$\frac{\partial\, rRM}{\partial\, RM}$
$0.3956^{\dagger}$	$0.4418^{\dagger}$	$0.5359^{\dagger}$	$0.5563^{\dagger}$	$4.2341^{\dagger}$	$0.1822^{\ddagger}$

$^{\dagger}[microV/V]/[lbs]$; $^{\ddagger}[microV/V]/[in\text{–}lbs]$.

Finally, it is interesting to examine the non–iterative part of the load iteration equation that is obtained after the application of the *Iterative Method*. The non–iterative part equals square matrix C_1^{-1} that is traditionally used to define the primary load iteration equation (see Ref. [6], App. 10 for more details). Table 14 below lists the values of matrix C_1^{-1} that were obtained from the calibration data set of the MK40B balance. In theory, these values should show good agreement with the thirty–six principle linear

Table 14: *Iterative Method* $\Longrightarrow$ Coefficients of square matrix ${C_1}^{-1}$. This matrix is the constant, i.e., non–iterative part of the load iteration equation.

	N1	N2	S1	S2	AF	RM
D1	2.535234e+00	2.778097e-01	-4.932499e-02	-9.880724e-03	1.315322e-03	9.730098e-03
D2	5.969601e-02	2.269548e+00	-3.205719e-03	-4.851284e-02	-1.416071e-03	-7.217468e-03
D3	-2.617729e-03	-1.766914e-02	1.867276e+00	7.809713e-02	1.554481e-03	1.617387e-03
D4	-3.263346e-03	7.638104e-03	2.555472e-02	1.798525e+00	-1.728196e-03	2.923631e-03
D5	2.406392e-06	5.540100e-06	-2.983715e-05	-2.341761e-05	2.361867e-01	3.783200e-03
D6	3.490554e-03	8.036107e-03	-4.327982e-02	-3.396806e-02	9.474557e-03	5.487663e+00

terms that were obtained after the application of the *Non–Iterative Method* to the calibration data (these coefficients are listed in Table 10). The values of Table 14 can be compared with the values of Table 10 by simply examining the ratio between two corresponding values. This ratio equals one if a value pair shows perfect agreement. The ratios of the thirty–six coefficients were computed. Then, the arithmetic mean of the ratios was determined. A mean value of 0.99998 was obtained (maximum of all ratios = 1.09915; minimum of all ratios = 0.849545). The mean value is very close to the value of 1.0 that describes perfect agreement between coefficient sets.

In summary, the comparison of different analysis results confirms that the load prediction accuracies of the *Non–Iterative* and the *Iterative Method* for the chosen *Task* balance calibration data set are the same for all practical purposes as long as (i) gage outputs are formatted as differences between a raw output and the natural zero of a gage, (ii) regression models with similar function classes are used for the analysis of the calibration data, (iii) regression models do not have invalid terms that cause unwanted dependencies, and (iv) a tare load iteration is performed.

VIII. Conclusions

Data from a six–component *Task* balance was analyzed in great detail. First, it was illustrated that absolute value terms are needed in both the regression models of the *Non–Iterative* and the *Iterative Method* so that *bi–directional* characteristics of the gages can be quantified. In addition, it is critical to format the electrical outputs of a *Task* balance as the difference between the raw output and the natural zero of a gage if the *Non–Iterative Method* is used to generate the load prediction equations.

Overall, the agreement between the load residuals, percent contributions, and primary sensitivities of the *Non–Iterative* and the *Iterative Method* is excellent. This observation confirms that the accuracy of the two balance load prediction methods is the same for all practical purposes if calibration data from a typical *Task* balance with *bi–directional* gage output characteristics is processed.

Acknowledgements

The author wants to thank Bob Gisler of NASA for his critical and constructive review of the paper. The work described in this paper was supported by the Wind Tunnel Division at NASA Ames Research Center under contract 80ARC022DA011.

References

[1] Galway, R. D., *A Comparison of Methods for Calibration and Use of Multi–Component Strain Gauge Wind Tunnel Balances,* National Aeronautical Establishment, National Research Council Canada – Conseil National de Recherches Canada, NRC No. 18227, Aeronautical Report LR–600, Ottawa, March 1980, p. 13, pp. 21–23, p. 27.

[2] Penrose, R., "On Best Approximate Solutions of Linear Matrix Equations," *Mathematical Proceedings of the Cambridge Philosophical Society*, Vol. 52, Issue 1, Jan. 1956, pp. 17–19.

[3] Baksalary, O. M., Trenkler, G., "The Moore–Penrose inverse: a hundred years on a frontline of physics research," *The European Physical Journal H 46, Article 9 (2021)*; Section 3, 2nd para.; Section 4, 1st para.; electronic copy ⟶ https://doi.org/10.1140/epjh/s13129–021–00011–y.

[4] AIAA/GTTC Internal Balance Technology Working Group, *Recommended Practice: Calibration and Use of Internal Strain–Gage Balances with Application to Wind Tunnel Testing*, *AIAA R–091A–2020*, revised/extended 2nd ed., sponsored & published by The American Institute of Aeronautics and Astronautics, Reston, Virginia, 2020, p. 16, pp. 19–24.

[5] Ulbrich, N., and Volden, T., "Regression Analysis of Experimental Data Using an Improved Math Model Search Algorithm," AIAA 2008–0833, paper presented at the 46th AIAA Aerospace Sciences Meeting, Reno, Nevada, January 2008, p. 4.

[6] Ulbrich, N., *Evaluation, Analysis, and Application of Internal Strain–Gage Balance Data*, NASA/CR–20210026455, contractor report, Jacobs Technology Inc., Moffett Field, California, December 2021.

[7] Hufnagel, K., *Wind Tunnel Balances*, 1st edition, Book Series: Experimental Fluid Mechanics, Springer International Publishing, 2022, p. 237.
